



Structural optimization of single-layer domes using surrogate-based physics-informed neural networks

Hongyu Wu^a, Yu-Ching Wu^{a,*}, Peng Zhi^a, Xiao Wu^a, Tao Zhu^a

^a Department of Structural Engineering, College of Civil Engineering, Tongji University, Shanghai, China

ARTICLE INFO

Keywords:

Structural optimization
metaheuristic
Single-layer domes
artificial bee colony algorithm
neural network surrogate-based model

ABSTRACT

This study aims at generation of a novel artificial bee colony algorithm using surrogate finite element method with neural network technique. In this paper, theory of surrogate finite element method with physics-informed neural networks (PINNs) are generated and applied to deal with the geometrically nonlinear optimization problem of size, shape and topology for single-layer domes. In the artificial bee colony algorithm, the feedforward neural network is used to surrogate finite element analyses. Three numerical examples of 10-bar truss, Lamella dome, and Kiewit dome are carried out to verify feasibility and accuracy of the proposed method. Results of the present study are in good agreement with ones from literature. It is indicated that optimization processes can be considerably accelerated using the modified algorithm. That is, using the neural network surrogate-based models could significantly increase computational efficiency of structural optimum design for single-layer domes.

1. Introduction

Structure optimization is one of the hottest issues of civil engineering. It has been very helpful to reduce time and cost of structural design. Main issue in structural design is to minimize weight of structures under certain constraints. It is important to investigate how to let weight of structures as light as possible with certain strength, stiffness and stability [1]. Structural optimization problems can be divided into three categories, size optimization, shape optimization and topology optimization [2]. Size optimization is a process to determine optimal section parameters of a component, such as area, moment of inertia, etc. In shape optimization, position of a joint is taken as a variable to optimize relative component position. In topology optimization, material properties are regarded as optimization parameters to find the best scheme in the structural design with the greatest flexibility.

Dome, as a specific style of structure, composed of a group of spatial rods with elegant shape and magnificent appearance. The special structural type could be used to cover a large area without too many columns, so it is widely used in theaters, gyms, and exhibition halls. In recent decades, steel has been widely designed as main material of dome structures. Compared with concrete, mechanical properties of steel structure are more stable and suitable for the specific structural style. In structural optimization process, domes need to be discretized as spatial beam elements and be analyzed using finite element method. Usually, most of joints are regarded as rigidly connected, and most of members are assumed to bear axial force and bending moment. Axial stiffness has been proved to be affected by the moment due to the large slenderness ratio [3]. In addition, overall stability of single-layer dome has been regarded as an important design index to evaluate buckling failure. Some studies have demonstrated that it might be necessary to take

* Corresponding author

E-mail address: ycwu@tongji.edu.cn (Y.-C. Wu).

<https://doi.org/10.1016/j.heliyon.2023.e20867>

Received 24 May 2023; Received in revised form 28 September 2023; Accepted 9 October 2023

Available online 14 October 2023

2405-8440/© 2023 The Authors. Published by Elsevier Ltd. This is an open access article under the CC BY-NC-ND license (<http://creativecommons.org/licenses/by-nc-nd/4.0/>).

geometric nonlinearity into account to accurately investigate global stability especially for light structures [4,5].

Solutions of structural optimization problems are gradient-based and search-based. Gradient-based optimization methods are usually based on ground structure technique, in which the structure initially contains a large number of joints and grids in design space. Subsets of the structure are selected from final solutions of iteration. For example, Changizi and Jalalpour have proposed an efficient gradient-based topology optimization framework for steel frames [6]. Mattias and Schevenels have proposed an gradient-based optimization algorithm to optimize the size, shape and topology of domes simultaneously [7]. It has been demonstrated that metaheuristic algorithms have great performance in search routine [8–10].

Metaheuristic algorithms are inspired from natural phenomena. Thus, it is used to solve optimization problems by imitating biological or physical situations [11]. They are divided into three categories, evolution-based, physics-based, and population-based. They have following advantages. At first, principle of algorithm is straightforward, and it is easy to understand and implement. Secondly, gradient is not required. Next, local optimal procedure is easily avoided. Also, they can be widely applied to many complex problems in different fields. Metaheuristic algorithms have been widely used in the field of building structure optimization, such as particle swarm optimization [12], genetic algorithm [2,13], ant colony algorithm [14,15], firefly algorithm [16–18], cuckoo search [19], harmony search [20], artificial bee colony algorithm [21–24], etc. As a subtopic of structure optimization, geometric nonlinear optimization design of dome structure has also been extensively investigated. Kaveh and Talatahari have applied charged system search to nonlinear optimal design of geodesic domes [25]. Richardson et al. have proposed form-finding technique based on dynamic relaxation and damping approach using genetic algorithm for geometric nonlinear shape optimization [26]. Çarba and Saka have generated a harmony search method for topology optimization of latticed domes [27]. Kaveh and Talatahari have presented a topology optimization method for several types of domes based on hybrid big bang–big crunch algorithm [3]. Kaveh and Javadi have proposed two chaotic firefly algorithm, chaos-based logistic firefly algorithms, and chaos-based Gaussian firefly algorithms, to optimize the nonlinear multi-frequency constrained domes [28]. Dede et al. have proposed series of Rao algorithms to optimize the size of small, medium and large-scale truss dome structures subjected to multiple dynamic frequency constraints [29].

In this paper, the artificial bee colony algorithm, one of the metaheuristic algorithms, is modified and applied to make geometrically nonlinear structural optimum design for single-layer steel domes. A surrogate-based deep neural network is proposed to replace finite element analyses in the optimization. Three numerical structural optimizations are conducted to verify feasibility and accuracy of the proposed approach. Results of the present study are in good agreement with ones from literature. It is indicated that the proposed algorithm significantly accelerates the optimization process with satisfied precision. That is, using the neural network surrogate-based models could significantly increase computational efficiency of topology optimum design for single-layer domes.

2. Theory of the surrogate finite element method

2.1. Computational scheme—Finite element method

Computational scheme of finite element method is defined as $C_{FEM}(u_i^h, w_i^h, v_i^h, g_i^h)$. In conventional continuum mechanics, the strong formulation of the partial differential equation is given in Eq. (1). Given $f_i: \Omega \rightarrow \mathbf{R}$, $g_i: \Gamma_{gi} \rightarrow \mathbf{R}$, and $t_i: \Gamma_{hi} \rightarrow \mathbf{R}$, find $u_i: \Omega \rightarrow \mathbf{R}$ such that

$$\begin{aligned} \sigma_{ij,j} + f_i &= 0 & \text{in } \Omega \\ u_i &= g_i & \text{on } \Gamma_{g_i} \\ \sigma_{ij}n_j &= t_i & \text{on } \Gamma_{h_i} \end{aligned} \tag{1}$$

where $\sigma_{ij} = c_{ijkl} \epsilon_{kl}$, $\epsilon_{kl} = u_{(k,l)} \equiv \frac{u_{k,l} + u_{l,k}}{2}$, ϵ_{kl} infinitesimal strain tensor, σ_{ij} Cauchy stress tensor, c_{ijkl} elastic coefficients, \mathbf{R} denotes the set of real numbers, Ω domain in \mathbf{R} , Γ boundary of Ω . Γ_{gi} and Γ_{hi} represent the specified boundary conditions, respectively; u_i denotes test functions; f_i , g_i , and h_i represent loading conditions.

The corresponding weak formulation of the partial differential equation is given in Eq. (2). Given \mathbf{f} , \mathbf{g} , and \mathbf{t} , in which $f_i: \Omega \rightarrow \mathbf{R}$, $g_i: \Gamma_{gi} \rightarrow \mathbf{R}$, and $t_i: \Gamma_{hi} \rightarrow \mathbf{R}$, for all $\mathbf{w} \in \mathbf{V}$ find $\mathbf{u} \in \delta$ such that

$$a(\mathbf{w}, \mathbf{u}) = (\mathbf{w}, \mathbf{f}) + (\mathbf{w}, \mathbf{t})_{\Gamma} \tag{2}$$

where

$$a(\mathbf{w}, \mathbf{u}) \equiv \int_{\Omega} w_{(i,j)} c_{ijkl} u_{(k,l)} d\Omega,$$

$$(\mathbf{w}, \mathbf{f}) \equiv \int_{\Omega} w_i f_i d\Omega,$$

$$(\mathbf{w}, \mathbf{t})_{\Gamma} \equiv \sum_{i=1}^{n_{sd}} \left(\int_{\Gamma_{\mathcal{E}_i}} w_i t_i d\Gamma \right)$$

Here δ denotes collections of trial solutions, \mathbf{V} collections of weighting functions, \mathbf{u} trial solutions, \mathbf{w} weighting functions. \mathbf{f} , \mathbf{g} , and \mathbf{h} represent body force, displacement, and traction vectors, respectively.

The corresponding Galerkin formulation of the partial differential equation is given in Eq. (3). Given \mathbf{f} , \mathbf{g} , and \mathbf{t} , in which $f_i: \Omega \rightarrow \mathbf{R}$,

$g_i: \Gamma_{gi} \rightarrow \mathbf{R}$, and $t_i: \Gamma_{hi} \rightarrow \mathbf{R}$, for all $\mathbf{w}^h \in \mathbf{V}^h$ find $\mathbf{u}^h = \mathbf{v}^h + \mathbf{g}^h \in \delta^h$ such that

$$a(\mathbf{w}^h, \mathbf{v}^h) = (\mathbf{w}^h, \mathbf{f}) + (\mathbf{w}^h, \mathbf{t})_\Gamma - a(\mathbf{w}^h, \mathbf{g}^h) \tag{3}$$

where δ^h and \mathbf{V}^h are finite-dimensional approximation to δ and \mathbf{V} ,

$$a(\mathbf{w}^h, \mathbf{v}^h) \equiv \int_\Omega w_{(i,j)}^h c_{ijkl} v_{(k,l)}^h d\Omega$$

$$(\mathbf{w}, \mathbf{f}) \equiv \int_\Omega w_i f_i d\Omega$$

$$(\mathbf{w}^h, \mathbf{t})_\Gamma \equiv \sum_{i=1}^{n_{sd}} \left(\int_{\Gamma_{s_i}} w_i^h t_i d\Gamma \right)$$

$$a(\mathbf{w}^h, \mathbf{g}^h) \equiv \int_\Omega w_{(i,j)}^h c_{ijkl} g_{(k,l)}^h d\Omega$$

Here h denotes element information; δ^h and \mathbf{V}^h represent test solutions and weighting functions, respectively; $\mathbf{u}^h, \mathbf{w}^h, \mathbf{g}^h$ denote virtual solutions, weighting functions, and boundary displacement in finite dimension, respectively.

2.2. Learning scheme—Deep neural network

Learning scheme of deep neural network is defined as $\mathbf{N}_{l=1}^L(\alpha; \mathbf{W}, \mathbf{b})$. Essentially, the neural network is composed of numerous neurons with adjustable connection weights. The Gaussian process is placed over the latent function $\mathbf{u}(\mathbf{x})$ given as Eq. (4).

$$\mathbf{u}(\mathbf{x}) \approx GP(0, k(\mathbf{x}, \mathbf{x}'; \theta)) \tag{4}$$

where θ denotes the hyper-parameters of the covariance function k , GP Gaussian process. Each neuron multiplies its initial input value by a certain weight, and adds other input values combined with other information values to the neuron. A sum is calculated and adjusted for deviation by the neuron. The output value is standardized using an excitation function. Neural networks are connected by different computing units layer by layer.

Let $\mathbf{N}_{l=1}^L(\alpha; \mathbf{W}, \mathbf{b}): \mathbf{R}^{d_x} \rightarrow \mathbf{R}^{d_y}$ be an L -layer neural network with input vector α , output vector β , and network parameters \mathbf{W}, \mathbf{b} . The feed-forward network generates information from one layer to the next layer through complex matrix calculation expressed in Eq. (5).

$$\mathbf{z}^l = \sigma^l(\mathbf{W}^l \mathbf{z}^{l-1} + \mathbf{b}^l) \quad l = 1, \dots, L \tag{5}$$

where \mathbf{z}^0 and \mathbf{z}^l present inputs and outputs of the network; \mathbf{W}, \mathbf{b} are weight and bias arrays; σ denotes activation function.

Artificial neural network is established in parallel and distributed form motivated by individual nervous system of human being. Multilayer feedforward neural network is used frequently in engineering applications. The elementary structure is composed of a group of input neurons, output neurons, and intermediate layer neurons. The neurons have the functions of receiving, transmitting and transforming. They receive a weighted value from the upper layer and transmit it to the lower layer through a specific activation function, as shown in Fig. 1(a and b).

The common activation function of neurons, including sigmoid: $y = \frac{1}{1+e^{-x}}$, tanh: $y = \frac{1-e^{-x}}{1+e^{-x}}$, and relu: $y = \max(0, x)$ functions, as shown in Fig. 2(a-c).

In the special structural form, the neural network is used to learn a certain number of data sets with similar characteristics, identify potential relationships, and generate either simple linear functions or complex nonlinear functions. The neural network technique has been widely used to solve complex problems which are difficult to be solved using conventional approaches such as pattern

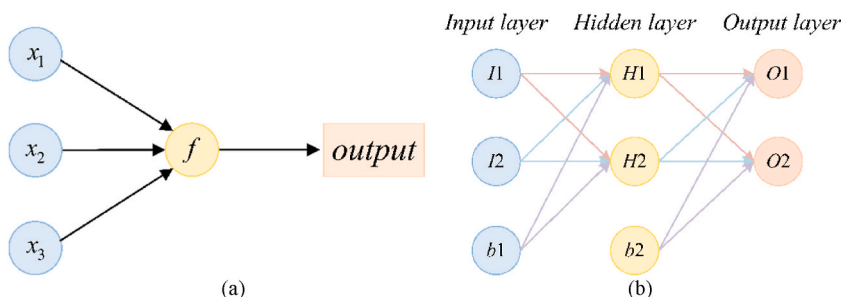


Fig. 1. Schematic diagram of (a) the neuron, and (b) the neural network model.

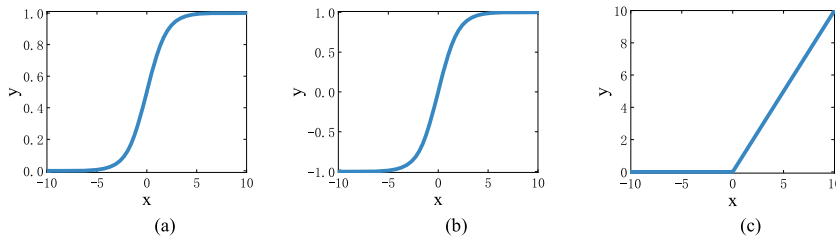


Fig. 2. Common activation functions: (a)sigmoid, (b)tanh, and(c)relu.

recognition, signal processing, knowledge engineering, expert system, optimization combination, robot control, etc.

2.3. Surrogate-based approach

The deep learning technique has been broadly investigated, and the surrogate approach has also been widely explored and applied in different areas [30]. But, corresponding mathematical theories seem to be limited. Meanwhile, researches on physical information neural networks are also well conducted. Based on conventional finite element theory, this study derives data-driven mathematical expressions of physical information neural networks to solve structural optimization problems.

The surrogate-based approach is simply defined as $C_{FEM} \leftarrow N_{l=1}^L$. It is indicated that the finite element computational schemes are replaced by the trained learning neural networks. For example, displacement vector and stress tensor in solid mechanics are defined in independent neural networks as our architecture of choice given in Eqs. (6) and (7).

$$u(x) \approx N_u^L(x^h) \tag{6}$$

$$\sigma(x) \approx N_\sigma^L(x^h) \tag{7}$$

And it can be done through the cost or the loss functions, denoted as *cost*, along with initial and boundary conditions as Eq. (8).

$$cost = |u - u^{*h}| + |u - u^{*h}|_{\partial\Omega} + |u_0 - u_0^{*h}| + |\sigma - \sigma^{*h}| + |a(w^h, v^h) - (w^h, f) - (w^h, t)_\Gamma + a(w^h, g^h)| \tag{8}$$

where u^{*h} denotes the solution of the Galerkin form within the domain Ω , u_0^{*h} the one at initial point. The *cost* represents residual from all given training points. The norm $|\bullet|$ of a generic quantity g defined in Ω domain is given as Eq. (9).

$$|g(x_i)| = \frac{1}{N} \sum_{i=1}^N g(x_i)^2 \tag{9}$$

where the x_i 's are the spatial points.

2.4. Physics-informed neural network (PINN)

Lately, physical information neural networks have been well developed by many researchers all over the world. Usually, it is used to deal with boundary value problems. However, this study explores how to use it deal with the structural optimization problems. This section generates the physical information neural network using rigorous mathematical formulation.

The physics-informed neural network is simply defined as $C_{PDE} \leftarrow N_{l=1}^L$, where PDE denotes partial differential equation. It is indicated that the computational scheme of partial differential equation, known as the strong form, is replaced by the trained learning neural network. Thus, we propose to have variables defined as independent neural networks as our architecture of choice in Eqs.10 and 11.

$$u(x) \approx N_u^L(x) \tag{10}$$

$$\sigma(x) \approx N_\sigma^L(x) \tag{11}$$

And it can be done through the cost or the loss functions, denoted as *cost*, along with initial and boundary conditions as Eq. (12).

$$cost = |u_i - u_i^*| + |u_i - u_i^*|_{\partial\Omega} + |u_0 - u_0^*| + |\sigma_{ij} - \sigma_{ij}^*| + |\sigma_{ij,j} + f_i| \tag{12}$$

Compared the surrogate-based approach, the physics-informed neural network technique makes direct measurements using the exact solution u_i^* instead of the approximated solution of the Galerkin form u^{*h} . Because it was proved that solutions of nodal points are of high precision, two methods could be almost identity.

3. Surrogate-based optimization schemes

The development of the first generation of computers was remarkable for their excellent computing power. At the same time, it has created a revolution in numerical methods. The finite element method was one of the most representative new methods at that time. In recent years, the era of artificial intelligence has arrived, and machine learning has made rapid progress, bringing about another revolution. For the field of computational mechanics, two methods are particularly valued. The first is the data-driven proxy method; The second type is physical information neural networks. These two methods have a certain degree of similarity, both of which use calculated numerical or analytical solutions to train deep neural networks. The goal of this study is to explore the feasibility and applicability of such methods in structural optimization problems.

The structural optimization problem is given as Eq. (13).

$$(SO) \begin{cases} \min_{\mathbf{x}, \mathbf{u}} g_0(\mathbf{x}, \mathbf{u}) \\ \text{s.t.} \begin{cases} \mathbf{K}(\mathbf{x})\mathbf{u} = \mathbf{F}(\mathbf{x}) \\ g_i(\mathbf{x}, \mathbf{u}) \leq 0, i = 1, \dots, l \\ \mathbf{x} \in \chi = \{ \mathbf{x} \in \mathbf{R}^n, x_j^{\min} \leq x_j \leq x_j^{\max}, i = 1, \dots, n \} \end{cases} \end{cases} \quad (13)$$

where $\mathbf{K}(\mathbf{x})$ is the global stiffness matrix of the structure, \mathbf{u} is the global displacement vector, and $\mathbf{F}(\mathbf{x})$ is the global external force vector. The displacements could be written as functions of the design variables in Eq. (14).

$$\mathbf{u}(\mathbf{x}) = \mathbf{K}^{-1}(\mathbf{x})\mathbf{F}(\mathbf{x}). \quad (14)$$

In general, the final finite element matrix form is always given as $\mathbf{K}(\mathbf{x})\mathbf{u} = \mathbf{F}(\mathbf{x})$. Thus, the structural optimization problem could be modified as Eq. (15).

$$(SO) \begin{cases} \min_{\mathbf{x}, \mathbf{u}} g_0(\mathbf{x}, \mathbf{u}) \\ \text{s.t.} \begin{cases} a(\mathbf{w}^h, \mathbf{v}^h) = (\mathbf{w}^h, \mathbf{f}) + (\mathbf{w}^h, \mathbf{t})_{\Gamma} - a(\mathbf{w}^h, \mathbf{g}^h) \\ g_i(\mathbf{x}, \mathbf{u}) \leq 0, i = 1, \dots, l \\ \mathbf{x} \in \chi = \{ \mathbf{x} \in \mathbf{R}^n, x_j^{\min} \leq x_j \leq x_j^{\max}, i = 1, \dots, n \} \end{cases} \end{cases} \quad (15)$$

The surrogate-based optimization scheme is $\mathbf{SO}(\mathbf{C}_{FEM} \leftarrow \mathbf{N}_{l=1}^L)$ expressed as Eq. (16).

$$(SO) \begin{cases} \min_{\mathbf{x}, \mathbf{u}} g_0(\mathbf{x}, \mathbf{u}) \\ \text{s.t.} \begin{cases} \mathbf{C}_{FEM} \leftarrow \mathbf{N}_{l=1}^L \\ g_i(\mathbf{x}, \mathbf{u}) \leq 0, i = 1, \dots, l \\ \mathbf{x} \in \chi = \{ \mathbf{x} \in \mathbf{R}^n, x_j^{\min} \leq x_j \leq x_j^{\max}, i = 1, \dots, n \} \end{cases} \end{cases} \quad (16)$$

It is indicated that the computational scheme of finite element analysis is replaced by the trained learning neural network.

For example, Kiewit and Lamella domes are commonly used structural styles as shown in Fig. 3(a and b). Main issue in structural design is to minimize weight of structures under certain constraints when boundary conditions are determined. There has been theoretical optimum design procedure of the dome structure to maintain stability of structural performance under different situations.

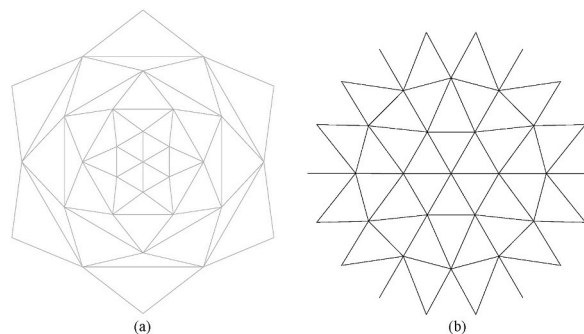


Fig. 3. Plan views of (a) Lamella dome, and (b) Kiewit dome.

In optimization of dome structures, dome center height (h), number of ribs (n), and section size (A_i) are assumed as optimization variables. Optimization objective is to minimize weight of the whole structure. According to China Code for Design of Steel Structures (GB50017-2017), maximum displacement (d), maximum stress (σ) and overall stability coefficient of the structure would be checked during the design process. In the optimization problem of dome structure, $x = \{h, n, DV_1, DV_2, \dots, DV_{ng}\}$, $g_0(x) = \sum_{i=1}^{ne} \rho_i A_i l_i$, and $g_i(x)$ include $(d_{max}/d_{lim}) - 1$, $(\sigma_{max}/\sigma_{lim}) - 1$, and $(\varphi/\varphi_{lim}) - 1$. Here x is optimization vector, h center height of dome, n number of ribs of domes, and DV_i the i^{th} group of member area. Other parameters are shown in Table 1 in details, where ng denotes number of member groups, $g_0(x)$ weight of structure. ρ_i density, A_i cross-sectional area, l_i length of the i^{th} member, ne number of elements, $g_i(x)$ constraints, d_{max} maximum joint displacement, σ_{max} maximum von Mises stress, φ overall stability coefficient of domes, and d_{lim} , σ_{lim} , φ_{lim} limitation of displacement, stress, and overall stability coefficient, respectively.

After design vectors are assigned to the platform, parametric modeling and nonlinear analysis are carried out to obtain structural response, including maximum joint displacement, maximum stress, and overall stability coefficient.

In the nonlinear finite element analyses, Timoshenko beam element is selected to compute displacement and stress of the dome structure. 1/300 of the maximum joint displacement is introduced into the structure as initial geometric defect. The arc-length method module is used to evaluate overall stability coefficient through iteration. The maximum iteration number of the arc length method is set as 30.

4. Artificial bee colony algorithms

The artificial colony algorithm has been proposed by Karaboga [31] at the first time. Then, it has been extensively investigated by researchers because of its rapid convergence, high optimization accuracy, few parameters, and simple principle. A series of modified methods have been proposed, for example, modified search equation of individual bees [32–37], modified quality of population initialization [38–40], combined with other meta-heuristic algorithms, such as genetic algorithm [41], ant colony algorithm [42,43], particle swarm optimization [44,45], etc. Because of symmetry of dome structures, number of optimization variables is countable. Thus, this paper adopts basic version of artificial bee colony algorithm combined with the artificial neural network technique, investigated in Section 4, to carry out the numerical experiments, introduced in Section 5.

Based on the clustering intelligence of natural organisms, various constrained and unconstrained optimization problems have been

Table 1
Available section list.

Type	Size						Section Area (cm ²)	Theoretical Weight(kg/m)	Inertia Moment Ix (cm ⁴)
	h(mm)	b(mm)	d(mm)	t(mm)	r(mm)	r1(mm)			
10	100	68	4.5	7.6	6.5	3.4	14.345	11.261	245
12.6	126	74	5	8.4	7	3.5	18.118	14.223	488
14	140	80	5.5	9.1	7.5	3.8	21.516	16.89	712
16	160	88	6	9.9	8	4	26.131	20.513	1130
18	180	94	6.5	10.7	8.5	4.3	30.756	24.143	1660
20a	200	100	7	11.4	9	4.5	35.578	27.929	2370
20b	200	102	9	11.4	9	4.5	39.578	31.069	2500
22a	220	110	7.5	12.3	9.5	4.8	42.128	33.07	3400
22b	220	112	9.5	12.3	9.5	4.8	46.528	36.524	3570
25a	250	116	8	13	10	5	48.541	38.105	5020
25b	250	118	10	13	10	5	53.541	42.03	5280
28a	280	122	8.5	13.7	10.5	5.3	55.404	43.492	7110
28b	280	124	10.5	13.7	10.5	5.3	61.004	47.888	7480
32a	320	130	9.5	15	11.5	5.8	67.156	52.717	11100
32b	320	132	11.5	15	11.5	5.8	73.556	57.741	11600
32c	320	134	13.5	15	11.5	5.8	79.956	62.765	12200
36a	360	136	10	15.8	12	6	76.48	60.037	15800
36b	360	138	12	15.8	12	6	83.68	65.689	16500
36c	360	140	14	15.8	12	6	90.88	71.341	17300
40a	400	142	10.5	16.5	12.5	6.3	86.112	67.598	21700
40b	400	144	12.5	16.5	12.5	6.3	94.112	73.878	22800
40c	400	146	14.5	16.5	12.5	6.3	102.112	80.158	23900
45a	450	150	11.5	18	13.5	6.8	102.446	80.42	22200
45b	450	152	13.5	18	13.5	6.8	111.446	87.485	33800
45c	450	154	15.5	18	13.5	6.8	120.446	94.55	35300
50a	500	158	12	20	14	7	119.304	93.654	46500
50b	500	160	14	20	14	7	129.304	101.504	48600
50c	500	162	16	20	14	7	139.304	109.354	50600
56a	560	166	12.5	21	14.5	7.3	135.435	106.316	65600
56b	560	168	14.5	21	14.5	7.3	146.635	115.108	68500
56c	560	170	16.5	21	14.5	7.3	157.835	123.9	71400
63a	630	176	13	22	15	7.5	154.658	121.407	93900
63b	630	178	15	22	15	7.5	167.258	131.298	98100
63c	630	180	17	22	15	7.5	179.858	141.189	102000

solved by imitating searching behavior of bees in process of collecting honey. Bee colonies in nature can be divided into three categories, employed bees, onlooker bees, and scout bees.

Each employed bee is associated with a food source. The employed bees evaluate quantity of food source and try to find better food source around it. After this search process is completed, the employed bees abandon the original food source and move to the other one. At the same time, the employed bees share information about the new food source with the bees in the hive through a waggle dance.

The hive receives all the food source information from the employed bees, evaluates and compares the qualities of all sources, and sends the onlooker bees in the hive to randomly select the food source. To better utilize and search for food source, onlooker bees tend to move to food source of high quality, and search around it to obtain another one.

If the better food source cannot be found after several times of searching around a current one, it would be abandoned and employed bees would be randomly changed to scout bees, in which new food sources would be randomly searched. After the search is completed, the scout bees would become employed bees, send information back to the hive, and cooperate with onlooker bees to start a new round of searching.

In the artificial bee colony algorithm, location of food source is design variable in the optimization process. Quality of food source is cost function of the design variable. Employed bees and onlooker bees account for half of the bee population, and they search for optimal or satisfactory solution in the solution space through information exchange and mutual cooperation.

The main steps of the artificial colony algorithm are given as follows: At first, food sources are initialized. For each food source, it is assigned to an employed bee. Secondly, employed bees search around food source. Next, quality of the new food source is evaluated and obtained by employed bees. And the current food source is replaced by the better one. Also, the onlooker bees evaluate quality of all food sources, move to a random food source by roulette algorithm, and update it. If no better food source is found in the neighborhood after several search attempts, the current one would be abandoned. And employed bees would automatically turn into scout bees and randomly assign a new food source. The previous four steps are repeated until the iteration is complete. The pseudocode of the artificial colony algorithm is shown in Algorithm 1.

```

    (Begin@Objective function  $f(X), X=(x_1, \dots, x_d)^T$ @Generate initial solutions of bees  $x_i$  ( $i = 1, 2, \dots, n$ )@Determine fitness function  $F_i$  of each bee@while( $t < \text{MaxGeneration}$ )@for  $i = 1:\text{num\_of\_employedbees}$ @Search around initial solutions@end@for  $i = 1:\text{num\_of\_onlookerbees}$ @Choose employed bees and follow@end@for  $i = 1:\text{num\_of\_scoutbees}$ @find better solutions@end@Rank and find best solution@end@Update global best solution@end)
    
```

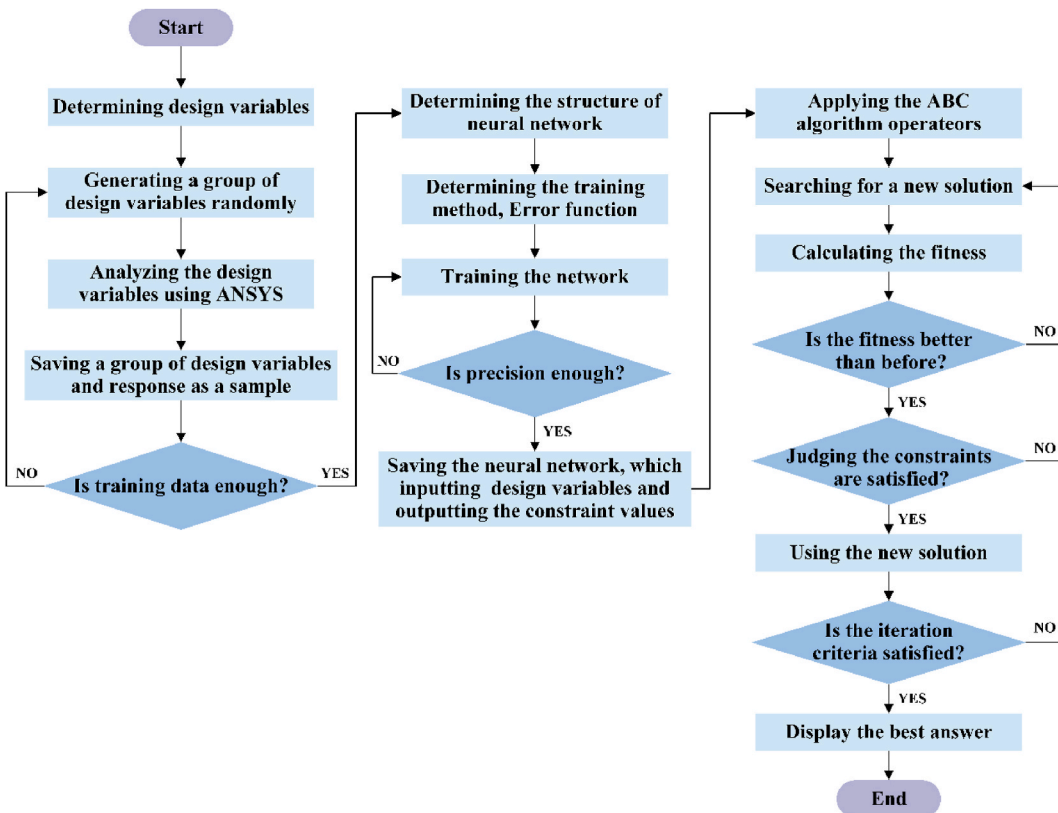


Fig. 4. Flowchart of the proposed optimization process.

Algorithm 1. The pseudocode of the artificial colony algorithm.

In structural optimization process with the metaheuristic algorithm, searching and verifying procedures are essential. Usually, finite element method (FEM) is used to verify structural constraints. However, for complex structural analyses, computational cost of the traditional method in the optimization process is very high. Thus, the artificial neural network could be a surrogate of finite element model potentially. After several numerical experiments are conducted, it is demonstrated that the artificial neural network technique could save about 50–80 times as much as computational cost of FEM to solve geometric nonlinear global stability problem of the single-layer steel dome structure.

In this paper, the modified artificial bee colony algorithm with surrogate-based neural network model is proposed. It consists of the following parts.

1. Structural responses are trained using the artificial neural network. The design variables are inputted into the artificial neural network, and the structural responses, including maximum joint displacement, maximum von Mises stress and overall stability coefficient, are outputted from the neural network. Sample features are randomly generated, and the finite element analyses are made, and sample labels are obtained. Number of samples is an important parameter of the training neural network. Too few samples will result in the overfitting of the neural network, while too many will cause the burden of finite element calculation. In this study, 3000–6000 training samples are generally taken.
2. In the optimization process of artificial bee colony algorithm, instead of using results from finite element analyses, we use ones predicted by the trained ANN to conduct the searching procedure.
3. To prevent inevitable errors of ANN, effective solutions judged by the neural network are recorded in the whole searching procedure as potential real optimal solutions. They are arranged in ascending order based on corresponding structural weight values. Then, finite element analyses are carried out. The minimum weight value under constraints is the final optimal solution of ABC-PINN.

The flowchart of the optimization method in this study is shown in Fig. 4. At first, sample data is initiated. According to the structural form, type and number of optimization variables are determined. Several groups of sample features are randomly generated and imported for structural analysis to obtain the sample labels. Secondly, the artificial neural network is trained. After the neural network structure training method, error function, and activation function are determined, the network error is reduced to fit the data. At last, the surrogate-based optimization is conducted, in which the finite element computation is surrogated by the trained ANN until iteration is finished.

5. Numerical experiments

In this section, a conventional 10-bar truss optimization is made to verify and validate efficiency and accuracy of the proposed method. Also, structural optimization of Lamella domes and Kiewit domes are carried out, in which geometric nonlinearity and overall stability are taken into account. Computational cost and accuracy of the proposed technique are made comparison with ones of conventional methods developed in literature.

5.1. 10-Bar truss optimization

Structural optimization of the 10-bar truss expressed in Fig. 5 is made to verify and validate efficiency and accuracy of the proposed method. It is a benchmark problem where No. 5 and No. 6 joints are connected by fixed hinged supports, No. 2 and No. 4 joints are subjected to a vertical downward force of 10^5 lb, and material density and elastic modulus are 0.1lb/in^3 and 10^4 ksi, respectively. The objective is to minimize weight of truss defined by Eq. (2). There are two constraints, maximum axial compression and tension stress of all structural members are limited to 25 ksi, and maximum displacement of joints in y direction is limited to ± 2 in. The discrete set of

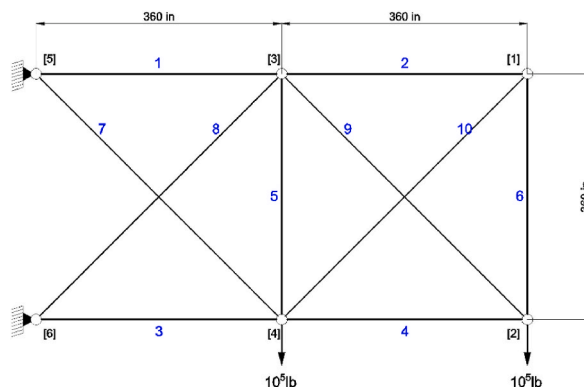


Fig. 5. The 10-bar truss.

sectional area in this example is given as $S = \{1.62, 1.8, 1.99, 2.13, 2.38, 2.62, 2.63, 2.88, 2.93, 3.09, 3.13, 3.38, 3.47, 3.55, 3.63, 3.84, 3.87, 3.88, 4.18, 4.22, 4.49, 4.59, 4.80, 4.97, 5.12, 5.74, 7.22, 7.97, 11.50, 13.50, 13.90, 14.20, 15.50, 16.00, 16.90, 18.80, 19.90, 22.00, 22.90, 26.50, 30.00, 33.5, 35, 37.5, 40, 42.5, 45, 47.5, 50, 52.5, 55, 57.5, 60, 62.5, 65, 67.5, 70, 72.5, 75, 77.5, 80, 82.5, 85, 87.5, 90\}(\text{in}^2)$.

In literature, several methods, such as Big Bang–Big Crunch Optimization(BB-BC) [46], Hybrid Harmony Search algorithm(HHS) [47], improved electro-search algorithm(IES) [48], have been adopted to optimize the 10-bar truss structure theoretically. The population number is set as 100, and the iteration number 1000. To make a comparison, two emerging swarm intelligence algorithms, Whale Optimization Algorithm(WOA) [49] and Grey Wolf Optimizer(GWO) [50] are used for the structural optimization problem.

In this study, cross-sectional areas of 10-bar truss components are used as features of the artificial neural network and imported into finite element analyses. Maximum joint displacement in y direction and maximum axial stress are used as labels of the ANN. 4000 groups of data samples are generated and normalized, in which the ratio of train, test and validation set is set as 7:1.5:1.5, and the probability distribution is always used during training. Levenberg-Marquardt approach is used as training technique with MSE as the error function, and sigmoid function is chosen as the activation function. The architecture of the network and its training results are presented in Fig. 6(a–c).

It is indicated that the neural network is converged after several hundred training sessions while fitting degree exceeds 99 %. The optimization result is shown in Table 2, and the convergence curve is shown in Fig. 7.

As shown in Fig. 7, GWO-PINN is converged rapidly, and ABC-PINN has the lightest solution. While the converged solution of ABC-FEM is worst, it might be resulted from that the neural network blurs the actual constraint boundary, meta-PINN is inclined to lighter solution whose FEM result might violate the constraints.

As shown in Table 2, ABC-PINN performs better than GWO-PINN and WOA-PINN in computational speed and accuracy. Compared with ABC-FEM, ABC-PINN only has 2.48 % in error, but the efficiency 3.99 % better than one of ABC-FEM.

From Table 2 and Fig. 8-9, it can be seen that the optimization of the cross-section of the 10-bar truss has the optimal solution, with

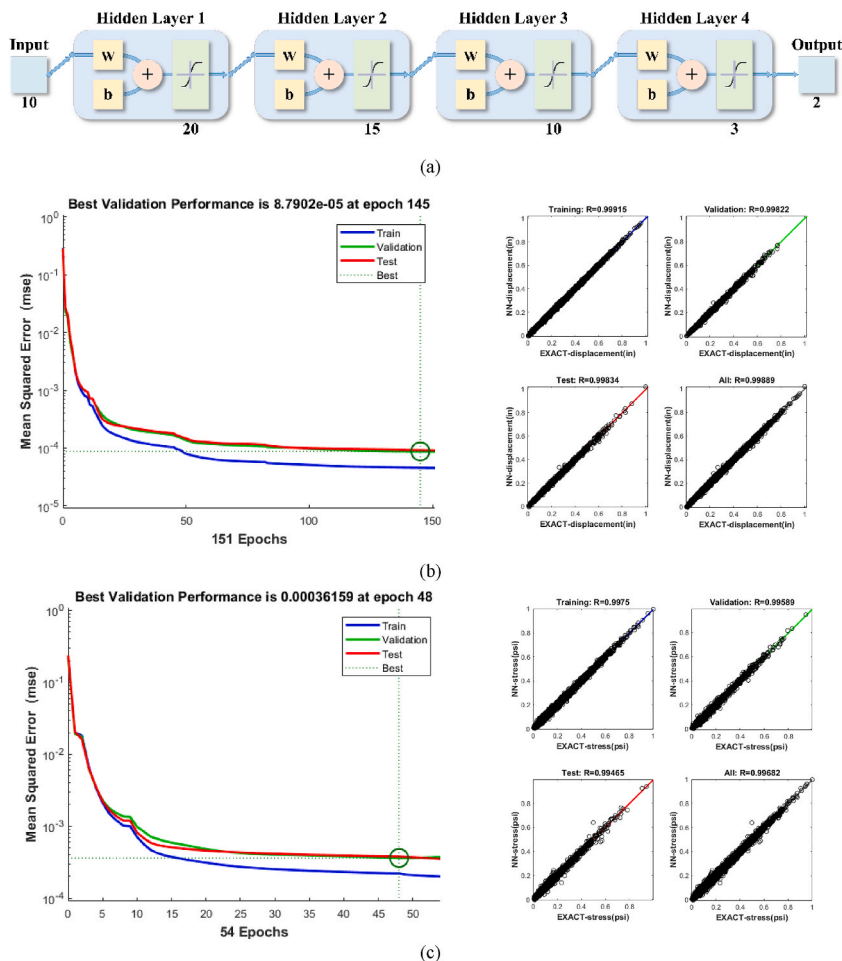


Fig. 6. Network structure for (a) and mean square error convergence curve and correlation regression for (b) the maximum nodal displacement, (c) the maximum principal stress.

Table 2
Optimization results for the 10-bar truss.

Design variables	BB-BC [8]	HHS [11]	IES [3]	The present study			
				ABC-FEM	ABC-PINN	GWO-PINN	WOA-PINN
DV1	33.50	33.50	33.50	33.50	30.00	45.00	22.00
DV2	1.62	1.62	1.62	1.62	1.62	1.62	1.62
DV3	22.90	22.90	22.90	22.90	22.00	19.90	15.50
DV4	14.20	14.20	14.20	14.20	22.90	15.50	19.90
DV5	1.62	1.62	1.62	1.62	1.62	1.99	2.38
DV6	1.62	1.62	1.62	1.62	2.38	1.62	2.93
DV7	7.97	7.97	7.97	7.97	7.97	5.12	14.20
DV8	22.90	22.90	22.90	22.90	22.00	22.90	30.00
DV9	22.00	22.00	22.00	22.00	22.00	22.90	37.50
DV10	1.62	1.62	1.62	1.62	1.62	1.99	1.62
Weight(lb.)	5490.74	5490.74	5490.74	5490.74	5627.08	5776.42	6557.84
FEM analyses	-	-	-	87948	1516	78	19
Data generation time(min.)	-	-	-	-	28.75	28.75	28.75
Training time(min.)	-	-	-	-	0.28	0.28	0.28
Optimization time(min.)	-	-	-	1921.45	47.58	76.93	116.56
Overall Time(min.)	-	-	-	1921.45	76.61	105.96	145.59

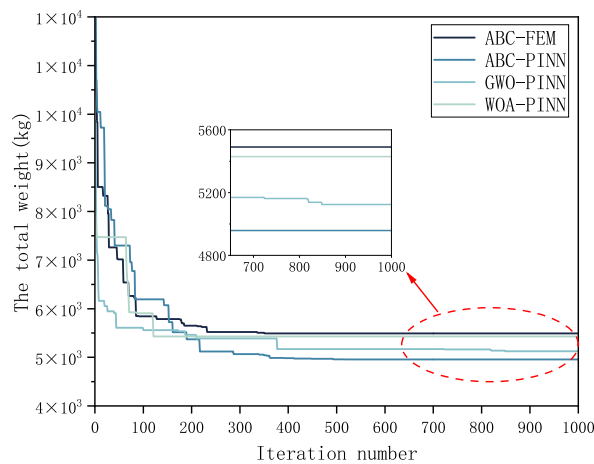


Fig. 7. Convergence curves of 10-bar truss: ABC-FEM, ABC-PINN, GWO-PINN, WOA-PINN.

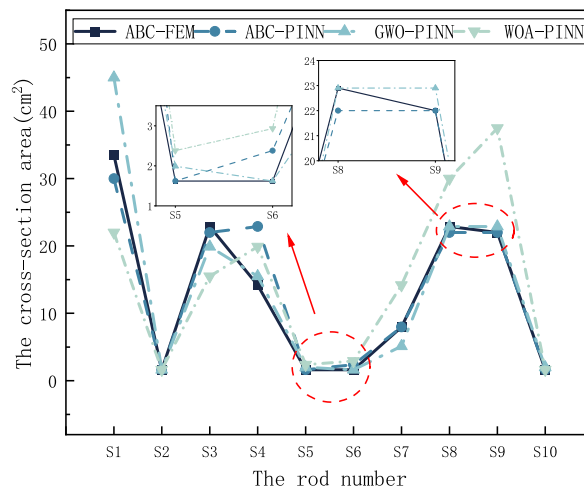


Fig. 8. A comparison among cross-section area of rods.

a structural weight of 5490.74 pounds. It is demonstrated that ABC-PINN has better performance for efficiency and accuracy than GWO-PINN and WOA-PINN. Compared with ABC-FEM, ABC-PINN, the total weight of the converged solution only lost 2.48 % of accuracy, but it reduces 96.01 % of computational time (see Fig. 9).

5.2. Lamella dome optimization

Fig. 10(a) presents the Lamella dome of 160 m in span, 40 m in center height. The spherical shape design is adopted. It is hinge-supported under 3 kN/m² of vertical distributed dead loading, 9.8 N/Kg of gravity loading, 2 kN/m² of vertical distributed live loading, and 1.5 kN/m² of horizontal distributed loading. Fig. 10(b) illustrates loadings and boundary conditions of this numerical example. Fig. 11(a–d) present the architecture of the network and mean square error convergence curve and correlation regression for the maximum nodal displacement, the maximum principal stress, and stability parameter.

According to design requirements of the dome structure, number of rings is set as 15, and number of ribs 20. Q345 steel is chosen with 345 MPa in yield strength. As shown in Table 1, sections are symmetrically distributed. Members 1–14 are circular in shape, and members 15–29 are longitudinal ribs. The displacement constraint is 0.4 m. 5000 sets of data samples are used for neural network training. They are normalized and randomly divided into train, test and validation set with the ratio of 7:1.5:1.5. Levenberg-Marquardt approach is used as training technique with MSE as the error function. The max epochs are set as 1000, and the learning rate is set as 0.01 sigmoid function is chosen as the activation function. Optimization results are shown in Table 3. The convergence curve is shown in Fig. 12.

As shown in Table 3, computational cost of ABC-PINN is less than ones of GWO-PINN and WOA-PINN. The computational time is around 69.38 % as much as one of ABC-FEM. However, GWO-PINN obtains the lowest error, 1.55 %.

In Fig. 13–14, compared with ABC-FEM, accuracy error of ABC-PINN is approximately 2.36 %, while running time decreases around 69.83 %; accuracy error of WOA-PINN about 1.55 %, while running time decreases around 60.83 %; accuracy error of GWO-PINN is approximately 21.52 %, while running time decreases around 65.65 %. It is demonstrated that ABC-PINN has better performance than other algorithms for computational accuracy and speed (see Fig. 14).

5.3. Kiewit dome

Fig. 15(a) presents a typical spherical Kiewit dome with 80 m in span. It is hinge-supported under 3 kN/m² of vertical distributed dead loading, 9.8 N/Kg of gravity loading, 1.5 kN/m² of vertical distributed live loading, and 1.0 kN/m² of horizontal distributed loading. Fig. 15(b) illustrates loading and boundary conditions of the Kiewit dome. Fig. 16(a–d) present the architecture of the network and mean square error convergence curve and correlation regression for the maximum nodal displacement, the maximum principal stress, and stability parameter.

According to requirements of the dome structural design, number of rings is set as 5. Q235 steel is used with 235 MPa in yield strength. The center height, *h*, is from 5 to 20 m. Members are uniformly distributed throughout the area, in which members 1–4 are circumferential rods, and members 5–9 are longitudinal rib rods. Displacement constraint is 0.2 m. 5000 sets of data samples are used for neural network training. They are normalized and randomly divided into train, test and validation set with the ratio of 7:1.5:1.5. Levenberg-Marquardt approach is used as training technique with MSE as the error function. The max epochs are set as 1000, and the learning rate is set as 0.01, sigmoid function is chosen as the activation function. Optimization results are shown in Table 3. The convergence curve is shown in Fig. 13.

Optimization results are presented in Table 4, and convergence curve is shown in Fig. 18.

As shown in Table 4, solutions of ABC-PINN are more efficient and accurate than ones of GWO-PINN and WOA-PINN. Error of ABC-PINN is approximately 8.20 % less than one of ABC-FEM. Computational cost ABC-PINN is approximately 11.73 % less than one of ABC-FEM.

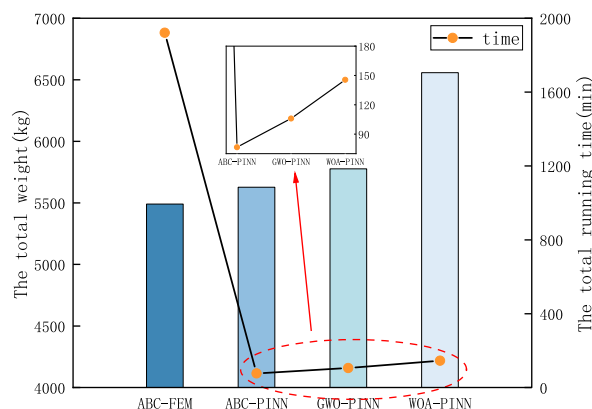


Fig. 9. A comparison of total weight and running time among different methods.

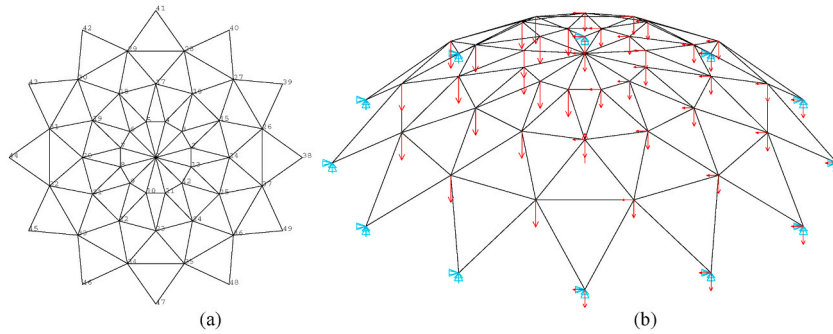


Fig. 10. (a) Plan view, (b) boundary conditions, and loading of Lamella domes.

As shown in Fig. 17, solutions GWO-PINN are converged rapidly. Solutions of ABC-PINN are relatively accurate. Solutions of WOA-PINN are converged quite slowly. It might have trapped in a locally optimal solution.

In Figs. 18–19, compared with ABC-FEM, accuracy error of ABC-PINN is approximately 8.20 %, while running time decreases around 88.27 %; accuracy error of WOA-PINN about 63.63 %, while running time decreases around 87.60 %; accuracy error of GWO-PINN is approximately 46.33 %, while running time decreases around 86.42 %. It is demonstrated that ABC-PINN has better performance than other algorithms for computational accuracy and speed.

5.4. Discussion

One might question about how to choose the architecture of the surrogate model and how many layers and neurons per layer. In this article, training finite element proxy networks is indeed an important part. Determining the type, structure, and various hyperparameters of neural networks is crucial for a good simulation result. In fact, we cannot theoretically determine the only optimal neural network model. In other words, multiple attempts and selection of the optimal solution may be inevitable. In this article, the structure of a neural network is determined by the number and characteristics of input neurons. The number of neurons in the first hidden layer is usually between one to two times the number of input neurons. And the number of neurons in each layer decreases sequentially with the number of layers. The number of neurons in the last layer of the hidden layer is also greater than the number of output neurons. Generally speaking, the fitting performance of neural networks improves with the increase of layers within a certain range. However, having more layers can also result in a loss of computational performance. In the size, shape, and topology optimization of dome structures, the number of layers of neural networks is often chosen from 3 to 5 based on the classification of input variables. As for the choice of super parameters such as activation function, loss function and learning rate, the method adopted in this paper is to give priority to several commonly used ones. In fact, they have shown satisfactory performance. It is worth mentioning that we also tried some other types of neural networks, such as convolutional neural network (CNN) and radial basis function neural networks (RBF). They did not show better performance than ANN.

The other issue is how to know when to stop collecting training data. It may be that the surrogate model is accurate in the early stage of the optimization, but gets less accurate as the optimization progresses. The explanation would be that too little training data can cause underfitting problems, and too much training data can increase computational burden and even bring about the risk of overfitting. We cannot theoretically determine how large a sample dataset is suitable and effective. Therefore, in the process of generating the sample dataset, we are based on the following principles: 1 Too little sample data can lead to insufficient accuracy. We usually hope that the fitting accuracy of neural network proxy finite element can reach over 95 %. If the fitting accuracy is too low, we tend to generate more sample data; 2. Generating too much sample data can lead to an increase in optimization costs. Sample data will not continue to be generated after the fitting accuracy meets the requirements.

Another question is that in Table 2, the proposed Ant Bee Colony optimization method requires a lot more FEM analyses but strangely the overall running time is shorter. A similar phenomenon occurs for the third example summarized in Table 4. For the second example, strangely only 1 FEM simulation is required for all the surrogate models. The plausible interpretations for this result could be that due to the non directionality of neural network errors, we cannot guarantee that the proxy results would meet the constraint conditions. Therefore, after the convergence of the meta heuristic algorithm, we perform finite element calculations on the reasonable solutions in its search path to ensure that the true mechanical solution of the final solution meets the constraint conditions. The main part of overall running time is the time required to generate sample data and the iteration time of meta heuristic algorithms. Although the ABC algorithm performs more finite element calculations, it is still better than the other two algorithms in terms of overall time and accuracy.

The next question is that why the study did not choose directly a consistent pure neural network solution as presented in literature [51,52]. According to our experiment, the amount of data required for using neural network to surrogate structure optimization algorithms is 105–1010 times greater than that of the proposed method in this paper. One of the main reasons is that in this study, the physical constraint conditions are given, rather than being used as input variables for neural networks. In other words, this article attempts to find a method that requires less data but still has high accuracy.

In addition, one might question why this study used the artificial bee colony algorithm in the optimization process. The rational

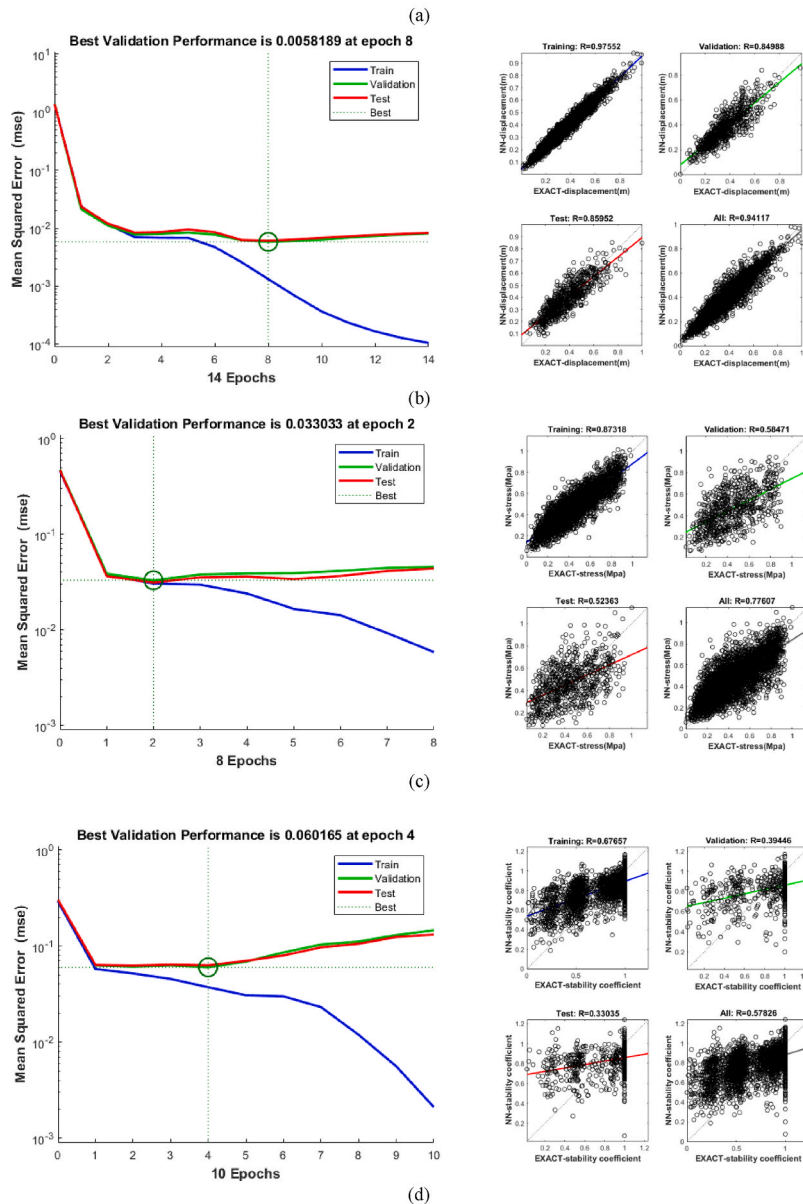
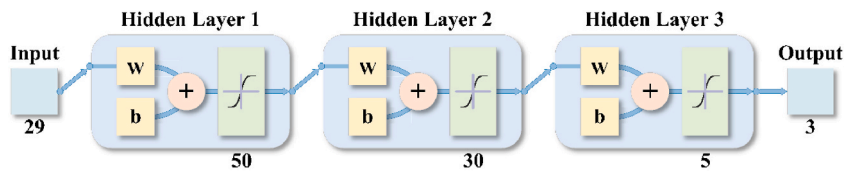


Fig. 11. The architecture of the network for (a) and mean square error convergence curve and correlation regression for (b) the maximum nodal displacement, (c) the maximum principal stress, and (d) stability parameter.

explanation would be that ABC is a very classic natural clustering algorithm. WOA and GWO are new meta heuristic algorithms that have received widespread attention in recent years. After comparison, ABC has shown better performance than the new algorithm in solving multi-scale optimization problems of dome structures. Thus, the application value of ABC has been demonstrated for solving practical problems.

Table 3
Optimization results for the Lamella dome.

Design variables	This study			
	ABC-FEM	ABC-PINN	GWO-PINN	WOA-PINN
DV ₁	36a	50b	63b	10
DV ₂	18	10	10	10
DV ₃	10	10	10	10
DV ₄	12.6	14	25a	32a
DV ₅	25a	25a	12.6	40a
DV ₆	20a	25a	28a	16
DV ₇	20b	18	14	32b
DV ₈	22a	28a	25a	28b
DV ₉	20b	22a	22a	36a
DV ₁₀	25a	25a	22a	28a
DV ₁₁	20b	25a	28a	25b
DV ₁₂	22a	18	22a	20a
DV ₁₃	22a	22a	22a	22a
DV ₁₄	22a	22a	22a	25b
DV ₁₅	20a	16	12.6	18
DV ₁₆	25a	22a	22a	14
DV ₁₇	20b	22a	18	22a
DV ₁₈	25b	25a	25a	28a
DV ₁₉	25a	20a	22a	22b
DV ₂₀	20a	20b	22a	28b
DV ₂₁	20a	22b	22a	25a
DV ₂₂	20b	22a	22a	25b
DV ₂₃	22b	22a	22a	14
DV ₂₄	20b	22a	22a	36a
DV ₂₅	22a	22a	22a	36a
DV ₂₆	22b	22a	22a	22b
DV ₂₇	18	22a	22a	20a
DV ₂₈	20b	20a	18	14
DV ₂₉	20a	22a	22a	28a
Best(Ib.)	280965.28	287586.79	285309.38	341422.16
FEM analyses	18662	1	1	1
Data generation time(min.)	–	297.25	297.25	297.25
Training time(min.)	–	2.18	2.18	2.18
Optimization time(min.)	1153.561	48.64	152.41	96.87
Overall Time(min.)	1153.561	348.07	451.84	396.30

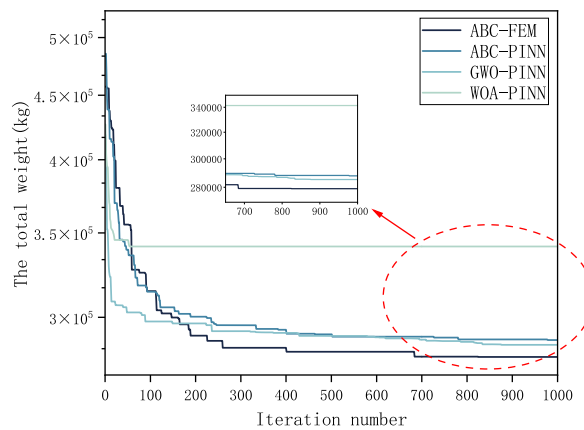


Fig. 12. Convergence curves of Lamella domes: ABC-FEM, ABC-PINN, GWO-PINN, WOA-PINN.

6. Conclusion

In this study, the novel artificial bee colony algorithm, in which finite element computation is replaced by trained neural network, is generated to make structural optimization for single-layer domes. At first, numerical experiment of the 10-bar truss is made. Results of the present study are in good agreement with ones from literature. Thus, feasibility and accuracy of the proposed artificial bee colony algorithm with surrogate-based neural network have been demonstrated. In addition, structural optimization of Lamella domes and Kiewit domes are carried out, in which geometric nonlinearity and overall stability are taken into account. Computational cost and

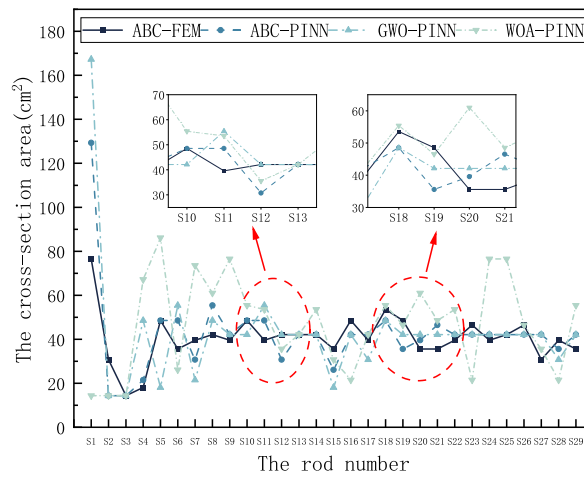


Fig. 13. A comparison among optimization parameters.

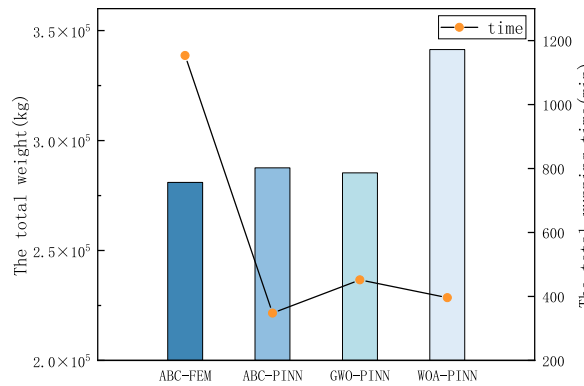


Fig. 14. A comparison of total weight and running time among different methods.

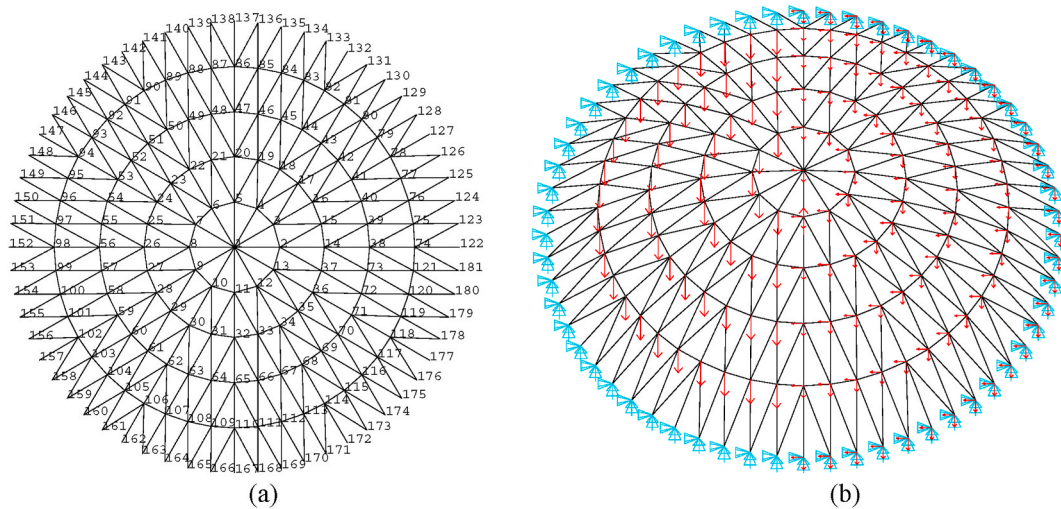


Fig. 15. (a) Plan view, (b) boundary conditions and loading of Kiewit domes.

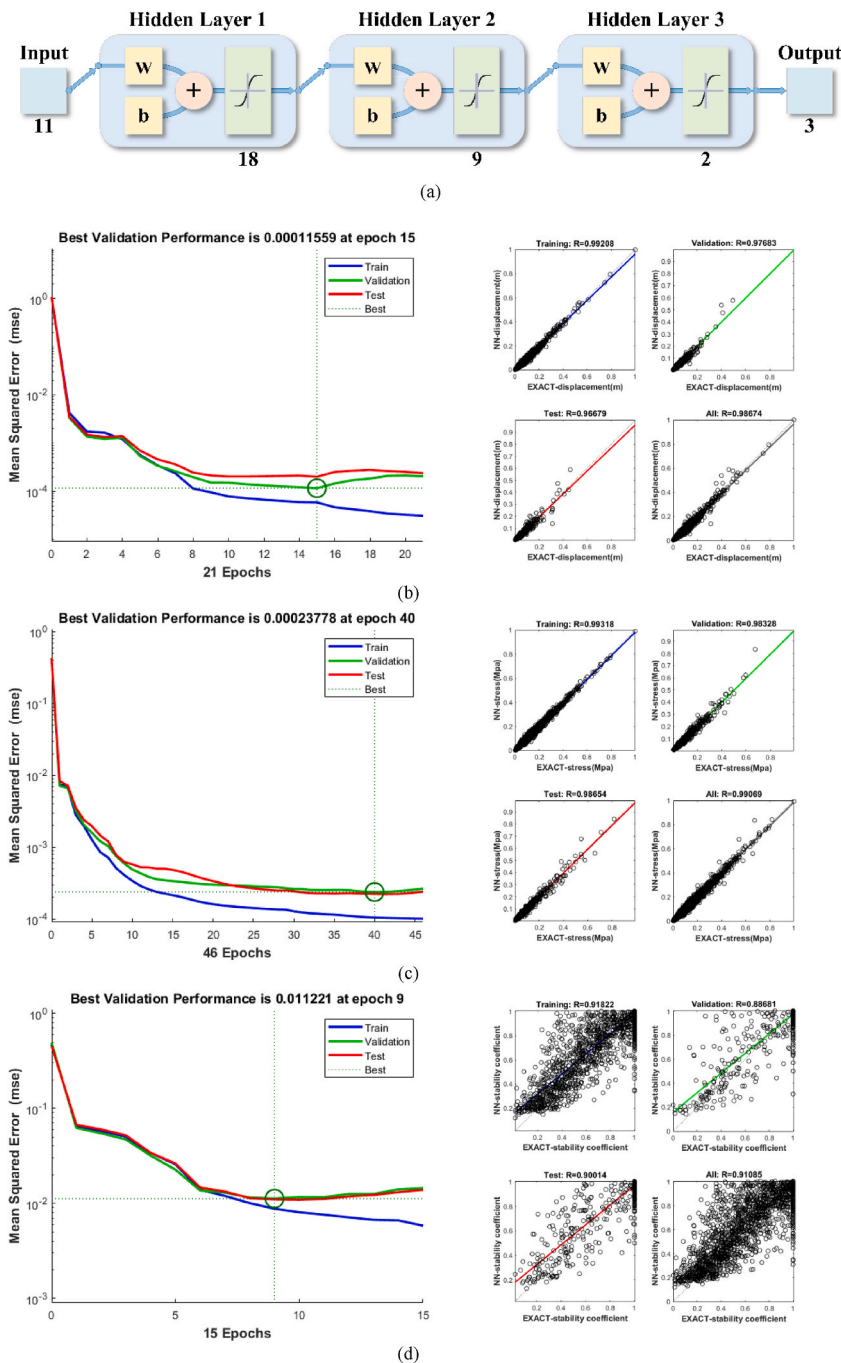


Fig. 16. The architecture of the network for (a) and mean square error convergence curve and correlation regression for (b) the maximum nodal displacement, (c) the maximum principal stress, and (d) stability parameter.

accuracy of the proposed technique are made comparison with ones of conventional methods developed in literature. It is indicated that the modified artificial bee colony algorithm with surrogate-based neural network model could increase convergence speed up to approximately 11.73 % with error averagely 2 % less than conventional approach. It is demonstrated that optimization processes can be considerably accelerated using the modified algorithm. That is, using the neural network surrogate-based models could significantly increase computational efficiency of topology optimum design for single-layer domes. After some modification, the novel artificial bee colony algorithm, in which finite element approaches are replaced by surrogate-based neural network techniques, could be easily extended to complex structures.

However, like most surrogate-based methods, this study does not consider the cost of modifying neural networks for higher

Table 4
Optimization results for the Kiewit dome.

Design variables	This study			
	ABC-FEM	ABC-PINN	GWO-PINN	WOA-PINN
h	19	19	16.5	15.25
n	6	6	6	6
DV ₁	18	20a	36a	40a
DV ₂	16	20a	22a	36a
DV ₃	14	18	10	20a
DV ₄	10	10	10	16
DV ₅	20a	20a	32a	22a
DV ₆	12.6	12.6	36b	16
DV ₇	16	14	36a	20a
DV ₈	16	18	32a	18
DV ₉	16	16	28a	22a
Weight(lb.)	42515.27	46002.84	69566.54	62212.87
FEM analyses	101150	100	200	27
Data generation time(min.)	–	416.57	416.57	416.57
Training time(min.)	–	2.89	2.89	2.89
Optimization time(min.)	3991.13	48.64	75.28	122.57
Overall Time(min.)	3991.13	468.10	494.74	542.03

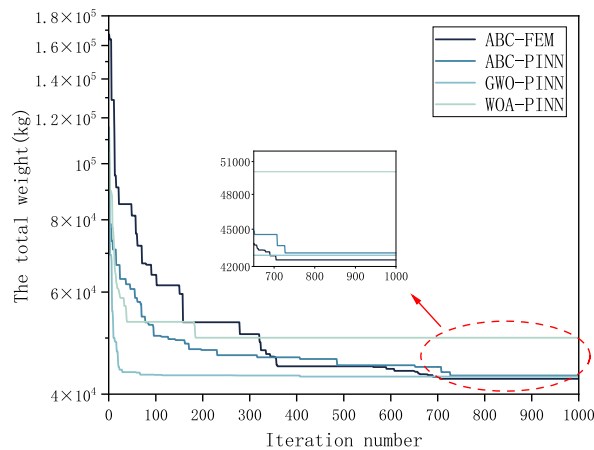


Fig. 17. Convergence curves of Kiewit dome: ABC-FEM, ABC-PINN, GWO-PINN, WOA-PINN.

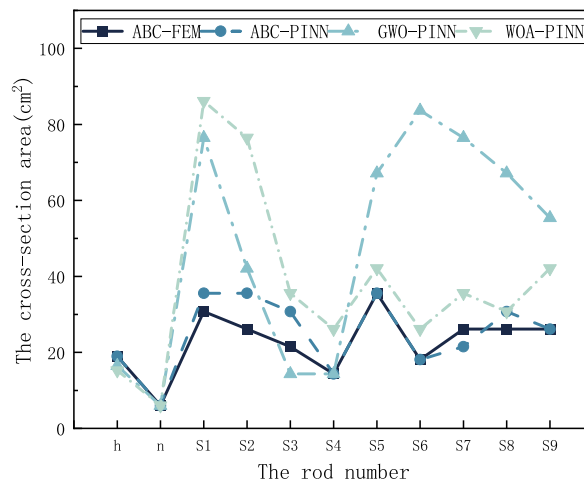


Fig. 18. A comparison among optimization parameters.

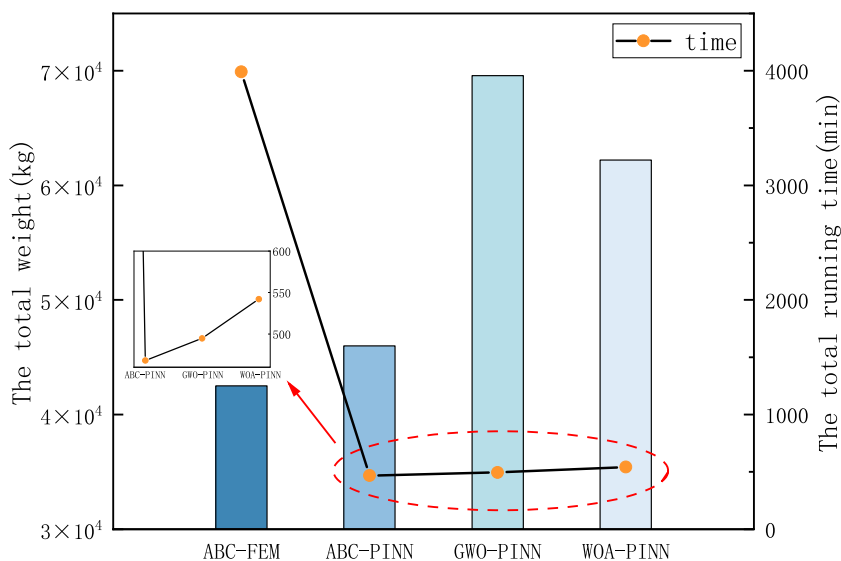


Fig. 19. A comparison of total weight and running time among different methods.

accuracy. In other words, if the cost of modifying neural network is taken into account, the whole computational cost would still exceed one of the conventional methods especially for some single and simple projects. Therefore, the method proposed in this study might need to cooperate with the certain project management technique to achieve its maximum benefits.

CRedit authorship contribution statement

Hongyu Wu: Formal analysis, Investigation, Methodology, Writing – original draft, Writing – review & editing. **Yu-Ching Wu:** Conceptualization, Funding acquisition, Project administration, Supervision, Writing – review & editing. **Peng Zhi:** Investigation, Methodology, Resources, Software, Validation. **Xiao Wu:** Data curation, Software, Validation, Visualization. **Tao Zhu:** Methodology, Software, Validation, Visualization.

Declaration of competing interest

The authors declare that they have no known competing financial interests or personal relationships that could have appeared to influence the work reported in this paper.

Acknowledgement

This work is sponsored by National Natural Science Foundation of China under grant 52178299. These supports are gratefully acknowledged. The authors also wish to thank Jesus Christ for listening our prayers and the anonymous reviewers for their thorough review of the article and their constructive advises.

References

- [1] M. Babaei, M. Sheidaii, Optimal design of double layer scallop domes using genetic algorithm, *Appl Math Mod* 37 (4) (2013) 2127–2138, <https://doi.org/10.1016/j.apm.2012.04.053>.
- [2] K. Deb, S. Gulati, Design of truss-structures for minimum weight using genetic algorithms, *Finis Ele in Anal and Des* 37 (5) (2001) 447–465, [https://doi.org/10.1016/S0168-874X\(00\)00057-3](https://doi.org/10.1016/S0168-874X(00)00057-3).
- [3] A. Kaveh, S. Talatahari, Optimal design of schwedler and ribbed domes via hybrid big bang-big crunch algorithm, *J of Const Steel Res* 66 (3) (2010) 412–419, <https://doi.org/10.1016/j.jcsr.2009.10.013>.
- [4] M.P. Saka, Optimum geometry design of geodesic domes using harmony search algorithm, *Adv in Struc Engin* 10 (6) (2007) 595–606, <https://doi.org/10.1260/136943307783571445>.
- [5] M.P. Saka, Optimum topological design of geometrically nonlinear single layer latticed domes using coupled genetic algorithm, *Comp & Struct* 85 (21–22) (2007) 1635–1646, <https://doi.org/10.1016/j.compstruc.2007.02.023>.
- [6] N. Changizi, M. Jalalpour, Topology optimization of steel frame structures with constraints on overall and individual member instabilities, *Finis Ele in Anal and Des* 141 (2008) 119–134, <https://doi.org/10.1016/j.finel.2017.11.003>.
- [7] W. Gythiel, M. Schevenels, Gradient-based size, shape, and topology optimization of single-layer reticulated shells subject to distributed loads, *Struc and Multi Opti* 2022 65 (5) (2022) 144, <https://doi.org/10.1007/s00158-022-03225-w>.
- [8] T.A. Nguyen, H.B. Ly, V. Tran, V. Predicting shear strength of slender beams without reinforcement using hybrid gradient boosting trees and optimization algorithms, *Fron of Stru and Civil Engi* 16 (10) (2022) 1267–1286, <https://doi.org/10.1007/s11709-022-0842-0>.
- [9] N. Pahnabi, S.M. Seyedpoor, Damage identification in connections of moment frames using time domain responses and an optimization method, *Fron of Stru and Civil Engi* 15 (4) (2021) 851–866, <https://doi.org/10.1007/s11709-021-0739-3>.

- [10] R. Rafiee, R. Shahzadi, H. Speresp, Structural optimization of filament wound composite pipes, *Fron of Stru and Civil Engi* 16 (8) (2022) 1056–1069, <https://doi.org/10.1007/s11709-022-0868-3>.
- [11] D.Q. Vu, F.E. Jalal, M. Iqbal, D.D. Nguyen, D.K. Trong, I. Prakash, B.T. Pham, Novel hybrid models of ANFIS and metaheuristic optimizations (SCE and ABC) for prediction of compressive strength of concrete using rebound hammer field test, *Fron of Stru and Civil Engi* 16 (8) (2022) 1003–1016, <https://doi.org/10.1007/s11709-022-0846-9>.
- [12] A. Baghdadi, M. Heristchian, H. Kloft, Design of prefabricated wall-floor building systems using meta-heuristic optimization algorithms, *Auto in Const* 114 (2020), 103156, <https://doi.org/10.1016/j.autcon.2020.103156>.
- [13] C. Lee, J. Ahn, Flexural design of reinforced concrete frames by genetic algorithm, *J of Stru Engi* 129 (6) (2003) 762–774, [https://doi.org/10.1061/\(ASCE\)0733-9445.2003.129:6\(762\)](https://doi.org/10.1061/(ASCE)0733-9445.2003.129:6(762)).
- [14] A. Kaveh, S. Talatahari, An improved ant colony optimization for the design of planar steel frames, *Engi Stru* 32 (3) (2010) 864–873, <https://doi.org/10.1016/j.engstruct.2009.12.012>.
- [15] C.V. Camp, B.J. Bichon, S.P. Stovall, Design of steel frames using ant colony optimization, *J of Stru Engi* 131 (3) (2005) 369–379, [https://doi.org/10.1061/\(ASCE\)0733-9445.2005.131:3\(369\)](https://doi.org/10.1061/(ASCE)0733-9445.2005.131:3(369)).
- [16] R.H. Lopez, A.J. Torii, L.F.F. Miguel, J.E.S. De Cursi, An approach for the global reliability based optimization of the size and shape of truss structures, *Mech & Indu* 16 (6) (2015) 603, <https://doi.org/10.1051/meca/2015029>.
- [17] A. Baghlani, M.H. Makiabadi, M. Sarcheshmehpour, Discrete optimum design of truss structures by an improved firefly algorithm, *Adva in Struc Engi* 17 (10) (2014) 1517–1530, <https://doi.org/10.1260/1369-4332.17.10.1517>.
- [18] W.M. Shaban, K. Elbaz, M. Amin, A.G. Ashour, A new systematic firefly algorithm for forecasting the durability of reinforced recycled aggregate concrete, *Fron of Stru and Civil Engi* 16 (3) (2022) 329–346, <https://doi.org/10.1007/s11709-022-0801-9>.
- [19] A.H. Gandomi, S. Talatahari, X.S. Yang, S. Deb, Design optimization of truss structures using cuckoo search algorithm, *The Stru Desi of Tall and Special Buil* 22 (17) (2013) 1330–1349, <https://doi.org/10.1002/ta.1033>.
- [20] M.P. Saka, Optimum design of steel sway frames to BS5950 using harmony search algorithm, *J of Cons Steel Res* 65 (1) (2009) 36–43, <https://doi.org/10.1016/j.jcsr.2008.02.005>.
- [21] M. Sonmez, Discrete optimum design of truss structures using artificial bee colony algorithm, *Stru and Mult Opti* 43 (1) (2011) 85–97, <https://doi.org/10.1007/s00158-010-0551-5>.
- [22] M.P. Saka, I. Aydogdu, Performance evaluation of artificial bee colony algorithm and its variants in the optimum design of steel skeletal structures, *Asian J of Civil Engi* 22 (1) (2021) 73–91.
- [23] F. Taheri, M.R. Ghasemi, B. Dizangian, Practical optimization of power transmission towers using the RBF-based ABC algorithm, *Stru Engi & Mech* 73 (4) (2020) 463–479, <https://doi.org/10.12989/sem.2020.73.4.463>.
- [24] J. Park, S. Han, Topology optimization for nonlinear structural problems based on artificial bee colony algorithm, *Inte J of Prec Engi and Manu* 16 (1) (2015) 91–97, <https://doi.org/10.1007/s12541-015-0011-7>.
- [25] A. Kaveh, S. Talatahari, Geometry and topology optimization of geodesic domes using charged system search, *Stru and Mult Opti* 43 (2) (2011) 215–229, <https://doi.org/10.1007/s00158-010-0566-y>.
- [26] J.N. Richardson, S. Adriaenssens, R.F. Coelho, P. Bouillard, Coupled form-finding and grid optimization approach for single layer grid shells, *Engi Stru* 52 (2013) 230–239, <https://doi.org/10.1016/j.engstruct.2013.02.017>.
- [27] S. Carbas, M.P. Saka, Optimum topology design of various geometrically nonlinear latticed domes using improved harmony search method, *Stru and Mult Opti* 45 (3) (2012) 377–399, <https://doi.org/10.1007/s00158-011-0675-2>.
- [28] A. Kaveh, S.M. Javadi, Chaos-based firefly algorithms for optimization of cyclically large-size braced steel domes with multiple frequency constraints, *Comp & Stru* 214 (2019) 28–39, <https://doi.org/10.1016/j.compstruc.2019.01.006>.
- [29] T. Dede, B. Atmaca, M. Grzywinski, R.V. Rao, Optimal design of dome structures with recently developed algorithm, *Rao series, Structures* 42 (2022) 65–79.
- [30] P. Zhi, Y. Wu, C. Qi, T. Zhu, X. Wu, H. Wu, Surrogate-based physics-informed neural networks for elliptic partial differential equations, *Math* 11 (2) (2023) 2723, <https://doi.org/10.3390/math11122723>.
- [31] D. Karaboga, An Idea Based on Honey Bee Swarm for Numerical Optimization, *Erciyes Univ., Kayseri, Turkey, Tech Rep-TR06*, 2005.
- [32] W.F. Gao, S.Y. Liu, L.L. Huang, A novel artificial bee colony algorithm based on modified search equation and orthogonal learning, *IEEE Trans. Cybern.* 43 (3) (2013) 1011–1024, <https://doi.org/10.1109/TSMCB.2012.2222373>.
- [33] A. Banharsakun, T. Achalakul, B. Sirinaovakul, The best-so-far selection in artificial bee colony algorithm, *Appl Soft Comp* 11 (2) (2011) 2888–2901, <https://doi.org/10.1016/j.asoc.2010.11.025>.
- [34] M.S. Kiran, H. Hakkı, M. Gunduz, H. Uguz, Artificial bee colony algorithm with variable search strategy for continuous optimization, *Info Sci* 300 (2015) 140–157, <https://doi.org/10.1016/j.ins.2014.12.043>.
- [35] W.F. Gao, F.T.S. Chan, L.L. Huang, S.Y. Liu, Bare bones artificial bee colony algorithm with parameter adaptation and fitness-based neighborhood, *Info Sci* 316 (2015) 180–200, <https://doi.org/10.1016/j.ins.2015.04.006>.
- [36] G. Li, P. Niu, X. Xiao, Development and investigation of efficient artificial bee colony algorithm for numerical function optimization, *Appl Soft Comp* 12 (1) (2012) 320–332, <https://doi.org/10.1016/j.asoc.2011.08.040>.
- [37] W. Gao, S. Liu, L. Huang, Enhancing artificial bee colony algorithm using more information-based search equations, *Info Sci* 270 (2014) 112–133, <https://doi.org/10.1016/j.ins.2014.02.104>.
- [38] H. Shayeghi, A. Ghasemi, A modified artificial bee colony based on chaos theory for solving non-convex emission/economic dispatch, *Ener Conv and Mana* 79 (2014) 344–354, <https://doi.org/10.1016/j.enconman.2013.12.028>.
- [39] C. Xu, H. Duan, F. Liu, Chaotic artificial bee colony approach to Uninhabited Combat Air Vehicle (UCAV) path planning, *Aero Sci and Tech* 14 (8) (2010) 535–541, <https://doi.org/10.1016/j.ast.2010.04.008>.
- [40] B. Alatas, Chaotic bee colony algorithms for global numerical optimization, *Expe Sys with Appl* 37 (8) (2010) 5682–5687, <https://doi.org/10.1016/j.eswa.2010.02.042>.
- [41] C. Ozturk, E. Hancer, D. Karaboga, A novel binary artificial bee colony algorithm based on genetic operators, *Info Sci* 297 (2015) 154–170, <https://doi.org/10.1016/j.ins.2014.10.060>.
- [42] M. Kefayat, A. Lashkar Ara, S.A. Nabavi Niaki, A hybrid of ant colony optimization and artificial bee colony algorithm for probabilistic optimal placement and sizing of distributed energy resources, *Energy Conv and Mana* 92 (2015) 149–161, <https://doi.org/10.1016/j.enconman.2014.12.037>.
- [43] V. Sundararaj, Optimal task assignment in mobile cloud computing by queue based ant-bee algorithm, *Wireless Personal Comm* 104 (1) (2019) 173–197, <https://doi.org/10.1007/s11277-018-6014-9>.
- [44] M.S. Kiran, M. Gündüz, A recombination-based hybridization of particle swarm optimization and artificial bee colony algorithm for continuous optimization problems, *Appl Soft Comp* 13 (4) (2013) 2188–2203, <https://doi.org/10.1016/j.asoc.2012.12.007>.
- [45] Z.Y. Li, W.Y. Wang, Y.Y. Yan, Z. Li, PS-ABC: a hybrid algorithm based on particle swarm and artificial bee colony for high-dimensional optimization problems, *Expert Sys with Appl* 42 (22) (2015) 8881–8895, <https://doi.org/10.1016/j.eswa.2015.07.043>.
- [46] C.V. Camp, Design of space trusses using big bang-big crunch optimization, *J of stru engi* 133 (7) (2007) 999–1008, [https://doi.org/10.1061/\(ASCE\)0733-9445.2007.133:7\(999\)](https://doi.org/10.1061/(ASCE)0733-9445.2007.133:7(999)).
- [47] M.Y. Cheng, D. Prayogo, Y.W. Wu, M.M. Lukito, A hybrid harmony search algorithm for discrete sizing optimization of truss structure, *Auto in Cons* 69 (2016) 21–33, <https://doi.org/10.1016/j.autcon.2016.05.023>.
- [48] A. Bigham, S. Gholizadeh, Topology optimization of nonlinear single-layer domes by an improved electro-search algorithm and its performance analysis using statistical tests, *Stru and Mult Opti* 62 (4) (2020) 1821–1848, <https://doi.org/10.1007/s00158-020-02578-4>.
- [49] S. Mirjalili, A. Lewis, The whale optimization algorithm, *Adva in Engi Soft* 95 (2016) 51–67, <https://doi.org/10.1016/j.advengsoft.2016.01.008>.

- [50] S. Mirjalili, S.M. Mirjalili, A. Lewis, Grey wolf optimizer, *Adva in Engi Soft* 69 (2014) 46–61, <https://doi.org/10.1016/j.advengsoft.2013.12.007>.
- [51] E. Samaniego, C. Anitescu, S. Goswami, V.M. Nguyen-Thanh, H. Guo, K. Hamdia, X. Zhuang, T. Rabczuk, An energy approach to the solution of partial differential equations in computational mechanics via machine learning: Concepts, implementation and applications, *Comp Meth in Appl Mech and Engi* 362 (2020), 112790, <https://doi.org/10.1016/j.cma.2019.112790>.
- [52] C. Anitescu, E. Atroshchenko, N. Alajlan, T. Rabczuk, Artificial neural network methods for the solution of second order boundary value problems, *Comput. Mater. Continua (CMC)* 59 (1) (2019) 345–359, <https://doi.org/10.32604/cmc.2019.06641>.